Natural variation in the *C. elegans* autophagy response and clearance of intracellular microsporidia

Keir M. Balla, Vladimir Lažetić, and Emily Troemel*

Division of Biological Sciences, University of California, San Diego, La Jolla, CA 92093 USA

*Lead contact: 9500 Gilman Dr #0349, La Jolla, CA 92093, etroemel@ucsd.edu

Keywords: autophagy, xenophagy, microsporidia, intestinal immunity, *C. elegans*, microsporidia, LGG-2, Atg8, LC3, natural variation

Word count: 7787 words

Abstract

Natural genetic variation can determine the outcome of an infection, and can reflect the co-evolutionary battle between hosts and pathogens. We previously found that a natural variant of the nematode *C. elegans* from Hawaii (HW) has increased resistance against natural microsporidian pathogens in the *Nematocida* genus compared to the standard laboratory strain of N2. Strikingly, HW animals can clear infection, while N2 animals cannot. HW animals can clear infection only at the first larval stage of life, which is when *Nematocida* imposes selective pressure on this host. Here we investigate how this clearance ability relates to xenophagy, which is the process of autophagy used for degrading intracellular microbes. We find there is much better targeting of autophagy machinery to parasites under conditions where they are cleared. In particular, ubiquitin targeting to *Nematocida* cells correlates very well with their subsequent clearance in terms of timing, host strain and age, as well as *Nematocida* species. Furthermore, clearance correlates with targeting of the LGG-2/LC3 autophagy protein to parasite cells, with HW animals having much more efficient targeting of LGG-2 to parasite cells than N2 animals. Surprisingly, however, we found that HW *lgg-2* mutants still can clear *Nematocida* infection, although they have increased pathogen load early in infection. These findings indicate that *lgg-2* regulates intracellular colonization of microsporidia inside intestinal cells, and a non-*lgg-2*-mediated process controls clearance. Thus, natural variation in xenophagy protein targeting correlates with, but is not required for clearance in this natural infection model.

Introduction

Natural genetic variation underlies differences in susceptibility to infection and inflammation among individuals.[1] Genome-wide association studies in humans have revealed genetic variation in innate immune genes that predispose individuals to increased risk of infection and autoimmune disease. For example, polymorphisms in autophagy genes Nod2, ATG16L, and IRGM are associated with increased risk for Crohn's disease, which is an inflammatory bowel disease characterized by a dysregulated gut microbiome.[2, 3] The discovery that natural variation in autophagy genes can lead to differences in inflammation is part of a large body of evidence indicating a close connection between inflammation, intestinal immunity, and autophagy.[4, 5]

Autophagy is a broadly conserved cellular process that was originally studied for its role in degrading and recycling bulk intracellular material, and subsequently has been shown to play a role in immunity.[6] When autophagy is used to degrade intracellular pathogens it is called xenophagy.[7-10] Xenophagy often begins with localization of host ubiquitin to intracellular microbes, followed by localization of autophagy proteins, formation of an autophagosome to enclose the microbe, and then fusion with a lysosome to degrade microbial cargo. Initial studies of the role for autophagy in immunity focused on xenophagy, although it is now appreciated there are 'non-canonical' forms of autophagy that also promote anti-microbial defense.[11] For example, autophagy can regulate secretion of anti-microbials outside the cell during stress.[12] Given that natural variation in autophagy underlies human risk of intestinal inflammatory disease, studying how autophagy responses vary among individuals in a species and how these responses contribute to immunity could provide insights into human disease.

The nematode *Caenorhabditis elegans* provides an attractive system for study of natural variation in innate immunity in the intestine and the role of autophagy.[13] There are many natural isolates of *C. elegans*, and various natural pathogens associated with these strains.[14] The most

common cause of infection for *C. elegans* in the wild is microsporidia, which comprise a phylum of >1400 species of obligate intracellular microbes related to fungi.[15, 16] Microsporidia invade host cells using a polar tube that 'fires' to deliver a parasite cell called a sporoplasm directly into the host cell. The first microsporidian species shown to infect *C. elegans* was isolated from wild-caught nematodes near Paris, France and we named it *Nematocida parisii* strain ERTm1 (nematode-killer from Paris), because it causes a lethal intestinal infection.[17] In the early stages of infection, *N. parisii* grows in direct contact with the host cytoplasm, and RNAseq analysis identified several predicted host ubiquitin ligase components induced by *N. parisii* infection.[18, 19] Because ubiquitin ligases can act upstream of autophagy by targeting ubiquitin to microbes exposed to the cytoplasm, we explored the role of autophagy/xenophagy in resistance to *N. parisii*. *C. elegans* has conserved autophagy machinery, and other studies have demonstrated a role for autophagy in response to infection with extracellular, clinically relevant pathogens.[13, 20-23] However, bona fide xenophagy (i.e. autophagy targeting to microbes that mediates subsequent clearance of pathogen) has not yet been demonstrated in *C. elegans*. In RNAi knock-down studies we found that autophagy is necessary and sufficient to regulate *N. parisii* load in the standard N2 laboratory strain of *C. elegans*, but only to a modest extent.[19] We did find a low level of autophagy targeting to parasites cells, but in subsequent studies we have shown that these animals are not able to clear infection.[19, 24] Thus, we do not find evidence for xenophagic clearance of pathogens in the N2 host strain.

In contrast to N2, we found that a natural variant of *C. elegans* from Hawaii (hereafter referred to as HW) does have the ability to clear microsporidia from its intestinal cells.[24] HW animals at the first larval stage can clear *Nematocida* infection, although they lose this ability later in life. In these previous studies we used a *Nematocida* strain (ERTm5) that we called *N. parisii* based on ribosomal sequence. We have subsequently performed whole genome sequencing and have

described ERTm5 as a new species because it has only an average 85% amino acid identity with *N. parisii*; we named this new species *Nematocida ironsii*.[25] Interestingly, the ability of HW to clear *N. ironsii* infection correlates with the developmental stage at which infection has fitness consequences for the host. Quantitative genetic analysis indicated that the HW genomic regions that confer increased immunity contain genes predicted to encode ubiquitin ligase adaptor proteins.[24] Therefore, we hypothesized that HW *C. elegans* may be better than N2 at targeting *Nematocida* cells with ubiquitin to direct autophagy machinery for clearance of these parasites via xenophagy. Indeed, because *C. elegans* lacks professional immune cells, and its intestinal epithelial cells are non-renewable, xenophagy provides an attractive candidate for a process that could explain how *C. elegans* can clear microsporidia infection from their intestinal cells.[26, 27]

Here we show natural variation in both the host and pathogen side in the *C. elegans* autophagy response to microsporidia, with a striking correlation between autophagy targeting to *Nematocida* cells and the ability to clear these pathogens from host intestinal cells. We find that HW animals have much higher levels of ubiquitin targeting to *Nematocida* cells compared to N2 animals. Furthermore, this targeting happens at the L1 stage, when HW have the ability clear infection, but not at the L4 stage, when HW cannot clear infection. We also find that ubiquitin targeting is more efficient to cells of a *Nematocida* species that is cleared, compared to two *Nematocida* species that are not cleared. In addition, we find much better targeting of the autophagy protein LGG-2/LC3 to *Nematocida* cells in HW animals compared to N2 animals. Surprisingly however, we find that LGG-2 is not required for clearance in HW animals, although it does affect pathogen load early during infection. Thus, *lgg-2* has an early role in regulating establishment of *Nematocida* inside intestinal cells, but is not important for clearing them via xenophagy. Altogether our findings show natural variation in xenophagic targeting to

microsporidia that are cleared from the *C. elegans* intestine, but the host appears to have separate, non-*lgg-2* related mechanisms for clearing this co-evolved pathogen.

Materials & Methods

C. elegans strains and maintenance

C. elegans were maintained on nematode growth medium seeded with *Escherichia coli* (OP50) as previously described.[28] The N2 and CB4856 (Hawaiian or HW in the text) strains were obtained from the CGC. All transgenic strains expressing fluorescent proteins carry extrachromosomal arrays. The N2 strain expressing GFP-tagged UBQ-2 (strain ERT261) was generated by injection of the pET341 plasmid *[vha-6p:::GFP::UBQ-2::unc-54 3'UTR, cb-unc-119(+)]* as previously described.[19] CB4856 animals were injected with pET341 to generate HW GFP::UBQ-2 animals (strain ERT337). To generate transgenic mCherry::GFP-tagged LGG-1 animals we injected N2 or CB4856 animals with the pMH878 plasmid from the Hansen lab *[lgg-1p::mCherry::GFP::LGG-1::lgg-1 3'UTR]*.[29] This yielded strains ERT426 and ERT429 in the CB4856 and N2 backgrounds, respectively. To generate transgenic GFP-tagged LGG-2 animals we injected QX1015 animals (*unc-119* mutant in CB4856 background) and bombarded EG6699 animals (*unc-119* mutant in N2 background) with the pRD117 plasmid from the Legouis lab *[lgg-2p::GFP::LGG-2::lgg-2 3'UTR::unc-119]*.[30] This yielded strains ERT496 and ERT511, respectively.

Nematocida infection assays and imaging

Infection experiments were performed with *N. ironsii* strain ERTm5, *N. parisii* strain ERTm1, and *N. ausubeli* strain ERTm2.[25, 31] Spores were prepared and quantified as previously described.[32] Host animals were either continuously exposed to *Nematocida* spores or pulse-inoculated with

spores for 3 hours as described in the figure legends. Infections of L1 stage animals or L4 stage animals were initiated as described previously.[24] Experiments were carried out at 20°C (Figures 1-4, S1B) or 25°C (Figures S1A, S4, S5). Animals were fixed at various times post-inoculation with 4% paraformaldehyde in PBS with 0.1% Tween 20 (PBST) for 45 minutes. N2, HW, GFP::UBQ-2 and GFP::LGG-2 transgenic animals were stained with the MicroB FISH probe conjugated to the CAL Fluor Red 610 dye at 5ng/µl overnight, then resuspended in PBST (clearance experiments) or Vectashield with DAPI (Vector Labs) to stain DNA (colocalization experiments). mCherry::GFP::LGG-1 animals were stained with the MicroB FISH probe conjugated to the Pacific Blue dye at 10ng/µl overnight, with no staining of DNA. For infection clearance experiments, the percentage of infected animals out of 100 total animals per sample was calculated as described previously.[24] To image the localization of transgenic proteins during *Nematocida* infections, fixed and stained animals were mounted on 5% agarose pads and imaged using a ×40 oil immersion objective on a Zeiss LSM700 confocal microscope run by ZEN2010 software. At least 10 infected transgenic animals were imaged per sample and *Nematocida* cells were counted as having transgenic proteins localized around them or not.

Measurements of transgenic protein levels

For Western blot measurements of protein levels, animals were washed off NGM plates with M9 buffer, and then washed once with PBS with 0.1% Tween 20 to remove bacteria. Samples were then resuspended in sample buffer with 1% SDS and 50 mM DTT and boiled at 95°C for 10 minutes. Lysates were then run on a 4-20% gradient SDS-PAGE gel (Bio-Rad) and transferred to PVDF membrane (Bio-Rad). The blots were stained with Ponseau S stain (Sigma-Aldrich) and imaged for total protein before staining with an anti-GFP antibody made in rabbits (a gift from Arshad Desai and Karen Oegema labs at UC San Diego) diluted at 1:5000 overnight at 4°C, then staining with an antirabbit HRP antibody at 1:10000 for 45 minutes at room

temperature. The blots were treated with ECL reagent (Amersham GE Healthcare Life Sciences) and imaged on a Bio-Rad ChemiDoc. For measurements of GFP protein levels in live animals, uninfected and *N. ironsii* infected animals were collected 15 hpi and measured on the COPAS Biosorter (Union Biometrica) for size (TOF) and GFP (green). More than 1000 animals were measured per sample. Animals expressing transgenic GFP were distinguished from non-expressing animals by measuring GFP levels in wild type N2 animals and only analyzing GFP levels in animals above this threshold.

CRISPR-Cas9 generation of *lgg-2* deletion alleles

Using the CRISPR design tool (http://crispr.mit.edu), DNA sequences with high scores were chosen in regions upstream from the start and downstream from the stop codon of *lgg-2* to create crRNAs (synthesized by Integrated DNA Technologies). crRNAs were annealed to the tracrRNA, and sgRNA products were co-injected with Cas9 protein and *dpy-10* sgRNA marker.[33] Dumpy F1 animals were screened for *lgg-2* deletions using PCR analysis. Isolated homozygous lines were confirmed and characterized by DNA sequence analysis and backcrossed three times to the original strain, CB4856. The *jy44* allele contains a 1376-nucleotide deletion, which removes the entire *lgg-2* gene and an additional 132 nucleotides upstream and 146 nucleotides downstream of the gene. Similarly, the whole *lgg-2* gene together with 138 nucleotides upstream and 146 nucleotides downstream (1382 nucleotides in total) are substituted for a single nucleotide insertion in *jy45* allele.

Feeding rate measurements

Fluorescent beads (Fluoresbrite ™ Polychromatic Red 0.5 μm Microspheres, Polysciences, Inc.) were added in 1:50 ratio to the mixes of starved L1 animals, OP50 food source and *N. ironsii* spores in M9 buffer, which were prepared following the protocol used in the clearance

experiments. After 30 minutes incubation at 25°C, animals were fixed in 4% paraformaldehyde and imaged using a Zeiss AxioImager. Fluorescence levels were analyzed using the FIJI program. Mean fluorescence per animal was calculated for 50 animals per strain, per replicate, in three separate experiments. Background fluorescence levels were subtracted from obtained results.

Results

N. ironsii cells are surrounded by ubiquitin more frequently inside the Hawaiian strain of *C. elegans* than the N2 strain

To investigate the hypothesis that HW *C. elegans* clear *N. ironsii* infections through improved targeting of ubiquitin to parasite cells followed by autophagic clearance, we examined the localization of ubiquitin to parasite cells in the HW host compared to the N2 host strain, which does not clear infections. First, we generated transgenic N2 and HW strains that express GFP-tagged ubiquitin under the control of an intestinal-specific promoter (GFP::UBQ-2). Ubiquitin is broadly conserved in eukaryotes,[34] and UBQ-2 encodes a canonical ubiquitin protein fused to the L40 ribosomal large subunit protein. We pulse-infected these GFP::UBQ-2-expressing strains at the first larval (L1) stage by feeding animals with *N. ironsii* spores for three hours, then removed them from spores and fixed them at different hours post-inoculation (hpi). We performed FISH staining on these fixed animals using a probe that targets *Nematocida* rRNA to label parasite cells and then determined the percentage of those cells that also have GFP::UBQ-2 localization (Figure 1A). With this method, we found that a much higher percentage of parasite cells had ubiquitin localization to parasite cells in HW animals than in N2 animals. For example, at 15 hpi 84% out of 19 parasite cells analyzed in 10 separate animals

had GFP::UBQ-2 targeting in HW animals (Figure 1B), and every animal had at least one parasite cell with GFP::UBQ-2 localization. In contrast, only 11% of parasite cells were targeted with GFP::UBQ-2 in N2 animals at 15 hpi (Figure 1B).

Next we analyzed how ubiquitin targeting to parasites correlates with their clearance. In previous clearance experiments at 25°C we had found parasite load much lower in HW animals at 20 hpi compared to 3 hpi, but did not measure when clearance began between those two timepoints.[24] Here we analyzed clearance at several timepoints after 3 hpi and saw that clearance begins around 10 hpi at 25°C (Figure S1A). 25°C is a slightly stressful condition for *C. elegans*, and autophagy is more active at this temperature. [35] We have also found that there are more proteins aggregates at this temperature, which can make localization experiments challenging,[19] so we have performed our autophagy localization experiments at 20°C (this paper and [19]). Therefore, we also analyzed clearance at 20°C to ensure that clearance is not just a high-temperature phenomenon, and to better compare the kinetics of clearance and ubiquitin targeting. We found that parasite clearance also occurs at 20°C (Figure S1B), indicating it is not specific to higher temperature. Furthermore, we were able to compare the kinetics of clearance with ubiquitin targeting at the same temperature, and found that the peak of ubiquitin targeting correlates with the start of clearance (compare Figure 1B and Figure S1B). These findings are consistent with ubiquitin targeting driving parasite clearance.

One potential explanation for increased targeting of ubiquitin to parasite cells in HW animals is increased expression from the GFP::UBQ-2 transgene in HW animals. To investigate this possibility, we compared protein levels of GFP::UBQ-2 with two methods. First, we performed Western blots with anti-GFP antibodies on lysates from transgenic HW and N2 animals to compare levels of GFP::UBQ-2 across populations of animals. Here we found that HW animals

do not have increased levels of GFP::UBQ-2 compared to N2 animals (Figure S2). Second, we analyzed GFP::UBQ-2 fluorescence on a per-animal level using a COPAS Biosort 'worm sorter'. While there was animal-to-animal variability in fluorescence levels of GFP-ubiquitin, the overall levels were not higher in HW compared to N2 animals (Figure 1C). Therefore, the increased targeting of GFP-ubiquitin to *N. ironsii* cells in HW compared to N2 does not appear to be simply due to increased GFP::UBQ-2 levels in HW animals.

Localization of ubiquitin to parasite cells correlates with their clearance in terms of host age and parasite species

In previous work, we showed that HW animals can clear infection by *N. ironsii* only during the first larval stage (L1), and this ability is lost in later larval stages.[24] To characterize genetic variation in clearance on the parasite side, we infected HW at the L1 and L4 stages with three different *Nematocida* species. We observed variation in clearance of these *Nematocida* species by HW animals, where *N. ironsii* was cleared by L1, but not L4 animals while *N. parisii* and *N. ausubeli* were cleared poorly by both L1 and L4 animals (Figure 2A, B). Therefore, the clearance of microsporidia by HW animals is specific to *N. ironsii* infections at the L1 stage.

To determine how these patterns of clearance related to the association of host ubiquitin with parasite cells, we examined the frequency of ubiquitin localization to *Nematocida* cells in L1 HW animals over time. Here we observed a high frequency of ubiquitin localization around *N. ironsii* cells but not *N. parisii* or *N. ausubeli* cells (Figure 2C). Furthermore, the high frequency of ubiquitin localization to *N. ironsii* cells was observed in HW animals infected at the L1 stage but not in HW animals infected at the L4 stage or N2 animals at either stage (Figure 2D). Thus, the frequency of host ubiquitin localization around microsporidia cells in *C. elegans* is highly correlated with clearance of infection.

Localization of LGG-2/LC3 but not LGG-1/GABARAP correlates with parasite clearance

Xenophagic clearance of intracellular pathogens involves targeting of autophagic machinery after ubiquitin targeting to pathogen cells. One of the most well-studied autophagic events is activation and conjugation of proteins in the LC3/GABARAP family to the developing autophagosome, which are required for fusion with the lysosome.[36] Therefore, we examined whether LGG-1 (homolog of GABARAP in mammals) or LGG-2 (homolog to LC3 in mammals), localized more frequently to parasite cells in HW worms compared to N2 worms. To analyze localization, we first generated N2 and HW transgenic animals with *lgg-1p::GFP::LGG-1* or *lgg-2::GFP::LGG-2* transgenes. Then we performed experiments similar to the ubiquitin studies in Figure 1. We pulse-infected these animals for 3 hours, fixed them at various timepoints after inoculation, stained with FISH to label *N. ironsii* cells and then quantified parasite localization with the GFP fusions (Figure 3A). Here we found that there was a gradual increase in GFP::LGG-1 targeting to *N. ironsii* cells over time in both N2 and HW animals, with no obvious difference between the two strains (Figure 3B). In contrast, we found that there was a much greater percentage of parasite cells targeted with GFP::LGG-2 in HW animals, compared with N2 animals (Figure 3B). This increased localization of LGG-2 was comparable to the increased ubiquitin targeting seen in HW compared to N2 (Figure 1B).

To eliminate the possibility that the increased targeting of LGG-2 in HW animals was simply due to increased levels of GFP::LGG-2 expression, we performed Western blot analysis (Figure S3) and COPAS Biosort 'worm sorter' analysis of GFP::LGG-2 (and GFP::LGG-1)(Figure 3C). Similar to our analysis of ubiquitin levels, we did not see an increased level of GFP::LGG-2 (or GFP::LGG-1) expression in HW compared to N2 animals. Additionally, we note that *N. ironsii* infection increased the levels of transgenic GFP::LGG-1 proteins in both N2 and HW strains

(Figure 3C). Infection with *N. parisii* does not lead to differences in mRNA expression of *lgg-1* (or *ubq-2* or *lgg-2*) based on RNAseq analysis, which suggests that the autophagy protein LGG-1 may be differentially regulated during microsporidia infection post-transcriptionally.

LGG-2/LC3 is not required for clearance, but does affect intracellular colonization of *N. ironsii* inside intestinal cells

The increased localization of LGG-2 to parasite cells in HW, and the ability of this strain to clear infection suggested that LGG-2 was important for the clearance ability in this strain. Therefore, we examined a functional role for LGG-2 in defense against *N. ironsii*. To do this we used CRISPR/Cas9 editing to generate a complete deletion of the *lgg-2* locus in the HW strain background. We isolated and characterized two independent alleles (called HW *lgg-2(jy44) and* HW *lgg-2(jy45)*) in which the entire *lgg-2* locus is deleted and should produce no LGG-2 protein (Figure 4A). We backcrossed these strains and then analyzed their ability to clear *N. ironsii*. In several independent experiments, we saw that HW *lgg-2* mutants were still able to clear *N. ironsii* between 3 hpi and 20 hpi (Figure 4B, Figure S2A). Therefore, despite the striking increase in localization of LGG-2 to *N. ironsii* cells in HW animals compared to N2 animals, LGG-2 is not required for clearance of *N. ironsii* under these conditions.

We did notice however, that HW *lgg-2* mutants had a higher initial dose of parasite at 3 hpi compared to wild-type HW animals. In particular, we saw that HW *lgg-2* mutants had a higher percentage of animals infected with *N. ironsii* compared to wild-type animals (Figure 4B, S4A). Furthermore, when we analyzed just the infected animals, we found that HW *lgg-2* animals had higher number of sporoplasms per animal (Figure 4C, S4B). One potentially trivial explanation for this difference could be that HW *lgg-2* mutants have greater exposure to the pathogen because it accumulates to a higher level within the intestinal lumen, either through increased

feeding or decreased defecation. To examine this possibility we used a fluorescent bead-feeding assay and measured accumulation of beads inside the intestinal lumen in HW and HW *lgg-2* mutants. Here we found that there was no increase in the accumulation of beads in HW *lgg-2* mutants, indicating that their increased parasite load at 3hpi is likely not due to increased exposure to parasites (Figure 4D; Figure S4C). Therefore, *lgg-2* may be acting at a very early stage to regulate pathogen load of the natural intracellular parasite *N. ironsii* in HW animals.

Although clearance still occurred in HW *lgg-2* mutants these animals had slightly less efficient clearance between 3 hpi and 20 hpi compared to HW wild-type animals. To determine whether this was due to the difference in initial dose at 3 hpi between HW and HW *lgg-2* mutants, we infected HW animals with a higher spore dose than HW *lgg-2* animals such that both strains had roughly equivalent initial sporoplasm number at 3 hpi (Figure S5). Under this condition, we found that clearance from 3 hpi to 20 hpi was similar in HW and HW *lgg-2* mutants, indicating that *lgg-2* is not required for clearance of *N. ironsii*, but is required for regulating the initial colonization of this natural parasite inside host intestinal cells.

Discussion

These studies demonstrate natural variation in *C. elegans* targeting of autophagy machinery to natural *Nematocida* pathogens, and show that targeting correlates very well with clearance of these pathogens (Figure 5). In particular, we found that HW animals, which can clear *N. ironsii* infection, have increased ubiquitin targeting to parasite cells compared to N2 animals, which cannot clear infection. Furthermore, this efficient targeting only occurs as the L1 stage when HW animals can clear infection, but not at the L4 stage when HW cannot clear infection. In addition, there is a correlation between clearance and localization of the autophagy protein LGG-2 to *N.*

ironsii cells in HW animals. Surprisingly however, we found that deletion of *lgg-2* in HW animals did not substantially alter the ability of this host to clear the parasite. In mammals there are six proteins in the LC3/GABARAP family involved in autophagy, three in the LC3 family and three in the GABARAP family, with redundancy among them.[36] *C. elegans* just has two proteins in this family, LGG-2 (homolog of LC3) and LGG-1 (homolog of GABARAP), and they do have redundant function in other contexts.[30, 37] Thus, it is possible that LGG-1 (GABARAP ortholog) is able to compensate for LGG-2 in clearance of microsporidia in HW *C. elegans*. Unfortunately, it is difficult to test this model, because LGG-1 is an essential gene, and HW worms are resistant to RNAi.[38] However, it seems somewhat unlikely that LGG-1 could substitute for LGG-2, given that there is extensive LGG-1 localization to parasite cells in N2 animals (at the equivalent level to HW animals, see Figure 3) and in this context LGG-1 is not sufficient for clearance.

How are *Nematocida* pathogens cleared from HW animals? Our findings do not rule out LGG-2 mediated xenophagy as playing a role in clearance, but they show it is not required. It is possible that LGG-2 does mediate clearance through xenophagy, and this process is redundant with another form of clearance (Figure 5). Given that *C. elegans* and *Nematocida* species appear to have a long co-evolutionary relationship,[15] it is possible that *C. elegans* evolved additional forms of clearance as part of an arms race between this host and its natural pathogen. Studies in other systems have described pathogen virulence factors that suppress host autophagy, for example through removing LC3 conjugation from the autophagosomal membrane.[9] Perhaps because another pathogen suppressed LGG-2-mediated autophagy in its evolutionary past, *C. elegans* evolved a separate pathway for clearance that functions here in the absence of LGG-2 to clear *N. ironsii*. Regardless of the reason, it is clear that HW animals have a pathway separate from LGG-2 that mediates clearance of *N. ironsii*. Given the extremely close correlation between ubiquitin targeting and *Nematocida* clearance (Figure 1-3), perhaps

ubiquitin is functionally relevant for this pathway, and serves to recruit another type of degradative machinery to the parasite in parallel to LGG-2. Unfortunately, because ubiquitin is an essential gene, it is difficult to test a functional role here. It is also possible that the ubiquitin targeting we see is not functionally relevant but is simply correlative with clearance. Indeed, there are several other studies where targeting of autophagic machinery to microbes is not indicative of a functional role in clearance.[10, 39] It is difficult to thoroughly test a role for autophagy in the clearance of *Nematocida* from HW animals, because many autophagy proteins are essential, and as mentioned above, RNAi knock-down in HW is relatively inefficient. Nonetheless, our findings suggest *C. elegans* evolved additional, non-xenophagic strategies for clearance of natural pathogens.

Interestingly, while *lgg-2* is not required for clearance, we found that HW animals defective in *lgg-2* do have more microsporidia sporoplasms inside intestinal cells compared to wild-type animals. These results indicate that *lgg-2* has a role in controlling early *Nematocida* colonization inside of intestinal cells, after the spores are ingested into the intestinal lumen. One explanation for these results is that *lgg-2* has a role in regulating the viability of microsporidia spores in the extracellular lumenal space, or in regulating their ability to fire the polar tube for invasion of intestinal cells. If so, this effect would be consistent with *lgg-2* acting through secretion of anti-microbial compounds, as has been shown for regulation of lysozyme secretion by the autophagy pathway in the mammalian intestine.[12] Another possibility is that *lgg-2* regulates the intracellular establishment of sporoplasms after they have been delivered into the cytoplasm by the polar tube. Nothing is known about whether the host cells control this stage of microsporidia infection, as polar tube firing is described as a mechanical rupture that 'forces' a parasite cell into the host cell.[16] However, it is exciting to consider that host cells may regulate this step.

Our observations that *lgg-2* control sporoplasm levels at 3 hpi are arguably the earliest stage at which a host factor has been shown to control microsporidia load in any system. Studies of microsporidia species that infect mammalian cells have implicated host glycosaminoglycans[40] and a transferrin receptor protein[41] in regulation of early steps, but the exact stage and mechanism by which they act is unknown. It will be interesting to further explore this early role for *lgg-2*. However, as polar tube firing has not been visualized in a live host it is difficult to determine whether *lgg-2* regulates polar tube firing or a later step in this live *C. elegans/Nematocida* system. Analysis in a tissue culture system might aid in distinguishing among these possibilities, although no such system exists for *C. elegans*. Thus, a role for the autophagy protein *lgg-2* in this very early step of sporoplasm colonization is intriguing but challenging to pursue further with existing tools. Nonetheless, the observations here paired with further analysis could shed light on the poorly understood question of how hosts control microsporidia infection.

Acknowledgements

We thank the Malene Hansen Lab, Arshad Desai/Karen Oegema labs and Renaud Legouis lab for reagents. We thank Cheng-Ju Kuo for technical support. We thank Malene Hansen, Robert Luallen, Johan Panek, Kirthi Reddy, Ivana Sfarcic, Eillen Tecle, and Ryan Underwood for comments on the manuscript.

Declaration of interest statement

This work was supported by NIH under R01 GM114139 and AG052622, and a Burroughs Wellcome Fund Investigators in the Pathogenesis of Infectious Diseases fellowship to ERT, and and a National Science Foundation Graduate Research Fellowship Program fellowship to KMB.

Figure Legends

Figure 1. Host ubiquitin protein UBQ-2 localizes around a greater percentage of *N. ironsii* cells in HW animals than in N2 animals.

(A) Example of UBQ-2 protein localized around *N. ironsii* cell in HW animal, fixed 10 hpi. *N. ironsii* cell (red FISH staining for rRNA) is shown in the first image, GFP-tagged transgenic host UBQ-2 protein (green) is shown in the second image, DNA stained with DAPI (blue) is shown in the third image, and a merged overlay is shown in the fourth image. The arrow points to *N. ironsii* cell. Scale bar = 5 μm. (B) Percentage of *N. ironsii* cells that have UBQ-2 localization at different timepoints. Each dot indicates the percentage of UBQ-2 localization around all *N. ironsii* cells in an experiment. Blue dots represent the frequencies observed in HW animals; red dots represent frequencies in N2 animals. Each experiment included analysis of at least 10

animals for HW and at least 25 animals for N2. Each animal infected by one to nine parasite cells. Data shown are compiled from more than three independent experiments per strain. (C) Analysis of GFP::UBQ-2 expression in N2 and HW strains with worm sorter. Transgenic GFP::UBQ-2 expression measured on an individual animal basis. AU, arbitrary units. Boxplots show the interquartile range (IQR) from 25th to 75th percentile with horizontal lines indicating medians. The range bars encompass all data within 1.5 IQR above and below the upper and lower IQRs, respectively. Dots show individuals outside of that range. Only GFP levels in GFP^+ animals are plotted, where GFP^+ includes all animals with GFP levels above non-transgenic N2 animals. More than 1000 animals were measured per strain and condition.

Figure 2. HW ability to clear microsporidia infection depends on host developmental stage and microsporidia species.

(A-C) Each dot represents an experiment, with similar parameters to Figure 1B. (A) HW L1 animals are more efficient in clearing *N. ironsii* infection (blue line), than *N. parisii* (green line) or *N. ausubeli* (purple line) infections. Animals were pulse-inoculated with spores of different *Nematocida* species, and the percent of infected animals (y-axis) was analyzed at different time points (x-axis). (B) HW animals infected at the L4 stage, using the same experimental setup as in (A), are unable to eliminate *Nematocida spp*. (C, D) The localization of host ubiquitin around *Nematocida spp.* cells is most frequent in contexts where infection is eliminated. (C) Transgenic GFP::UBQ-2 HW L1 animals were pulse-inoculated with *Nematocida spp.* spores and fractions of the population were fixed at several time points afterwards to assess the frequency of UBQ-2 localization around *N. ironsii* (blue line), *N. parisii* (green line), or *N. ausubeli* (purple line) cells. Data shown are representative of two independent experiments. (D) Transgenic GFP::UBQ-2 N2 and HW animals were inoculated with *N. ironsii* spores at the L1 stage or L4 stage and fixed 10 hpi to quantify the frequency of UBQ-2 localization around *N. ironsii* cells. Data for L1

infections are from six independent experiments, data for L4 infections are from two independent experiments. Averages are shown with standard deviations. (A-D) All experiments were carried out at 20°C.

Figure 3. Host autophagy proteins LGG-1 and LGG-2 localize around microsporidia cells with distinct patterns in the resistant HW strain and susceptible N2 strain.

(A) Examples of autophagy host proteins LGG-1 and LGG-2 localized around *N. ironsii* cells. The upper row shows mCherry-tagged transgenic host LGG-1 (red) in the first column, GFP-tagged transgenic host LGG-1 (green) in the second column, *N. ironsii* (blue) in the third column, and a merged image in the fourth column. The lower row shows *N. ironsii* FISH staining for rRNA (red) in the first column, GFP-tagged LGG-2 (green) in the second column, DNA stained with DAPI (blue) in the third column, and a merged image in the fourth column. Scale bars = 5 μm. The arrows point to *N. ironsii* cells. The images for mCherry::GFP::LGG-1 were from transgenic HW animals fixed 16 hpi and for GFP::LGG-2 12 hpi. (B) Percentage of *N. ironsii* cells with localization of host transgenic fusion proteins (LGG-1 in the upper graph, LGG-2 in the lower graph) over time. Each dot represents an experiment showing average frequency of localization around more than 10 *N. ironsii* cells per sample, with at least 10 animals per experiment. Blue dots represent the frequencies observed in HW animals; red dots represent frequencies in N2 animals. Data shown are compiled from more than three independent experiments per strain. (C) GFP-fusion autophagy protein analysis in transgenic N2 and HW strains. Transgenic GFP expression measured on an individual animal basis. AU, arbitrary units. As in Figure 1, boxplots show the interquartile range (IQR) from 25th to 75th percentile with horizontal lines indicating medians. The range bars encompass all data within 1.5 IQR above and below the upper and lower IQRs, respectively. Dots show individuals outside of that range. Only GFP levels in GFP^+ animals are plotted, where GFP^+ includes all animals with GFP levels

above non-transgenic N2 animals. More than 1000 animals were measured per strain and condition.

Figure 4. LGG-2 is not required for *N. ironsii* clearance, but does regulate early intracellular colonization in HW *C. elegans*.

(A) Schematic representation of *lgg-2* gene. Orange boxes indicate exons, gray boxes indicate UTRs. The red lines mark deletion allele *jy44* and indel allele *jy45* (inserted thymidine is indicated in the red circle). (B) *N. ironsii* clearance in N2 wild-type (wt) animals (gray lines), HW wild-type (wt) (green lines) and HW *lgg-2* mutant animals (orange lines). Thick lines represent average values of six experiments; dotted lines indicate results from individual experiments. 100 animals were analyzed per strain per time point (3 hpi and 20 hpi). (C) HW *lgg-2* mutants on average have significantly higher *N. ironsii* colonization in comparison to HW wild-type animals, and similar infection rate to N2 animals, under the same experimental conditions. Results from six independent experiments are shown as box-and-whisker plots, indicating the number of *N. ironsii* sporoplasms per animal at 3 hpi. Each box represents 50% of the data closest to the median value (line in the box). Whiskers span the values outside of the box. More than 400 animals were analyzed for each strain. Uninfected animals were excluded. A student's t-test was used to calculate *p* values; $p<0.001$ is indicated with four asterisks; ns indicates non-significant difference ($p>0.05$). (D) Fluorescent bead accumulation in the intestines of infected L1 animals after 30 minutes. AU, arbitrary units. HW *lgg-2(jy44)* mutants do not show increased feeding rate in comparison to wild-type HW animals. Average red fluorescence intensities per whole animal are shown in arbitrary units (AU) on y-axis. Each dot represents one animal. The analysis was done in 50 animals per strain in three replicates. A student's t-test was used to calculate *p* values; ns indicates non-significant difference ($p > 0.05$). (B-D) All experiments were performed at 25°C.

Figure 5. Model for invasion and clearance of *N. ironsii* in HW *C. elegans* hosts

N2 *C. elegans* fail to clear *N. ironsii* infection, while HW *C. elegans* clears *N. ironsii* as L1 animals, when there is high ubiquitin and LGG-2 targeting. An LGG-2-independent pathway mediates clearance, and LGG-2 inhibits initial establishment of *N. ironsii* inside host intestinal cells.

Figure S1. Clearance of *N. ironsii* infections occurs gradually over time in HW animals at both 25°C and 20°C.

(A) HW L1 animals were pulse-inoculated with *N. ironsii* spores and fractions of the population were fixed at several time points afterwards to assess the frequency of infection. Experiments were carried out at 25°C. Data from three independent experiments are shown in blue lines. (B) Same experimental setup described above in (A), only the experiment was carried out at 20°C.

Figure S2. GFP::UBQ-2 fusion Western blot analysis in transgenic N2 and HW strains. (A) Proteins were extracted from uninfected and *N. ironsii* infected animals (15 hpi) and analyzed by SDS-PAGE followed by Western blot using an anti-GFP antibody. Background staining of proteins from non-transgenic infected animals is shown in the last two columns. The predicted size of GFP::UBQ-2 is 35.4 kD. (B) Loading of all proteins per sample visualized by Ponceau S staining.

Figure S3. GFP::LGG-1 and GFP::LGG-2 fusion Western blot analysis in transgenic N2 and HW strains. (A) Proteins were extracted from uninfected and *N. ironsii* infected animals (15 hpi) and analyzed by SDS-PAGE followed by Western blot using an anti-GFP antibody (upper gel). Background staining of proteins from non-transgenic infected animals is shown in the last

two columns. The predicted size of GFP::LGG-1 is 70.4 kD and the predicted size of GFP::LGG-2 is 43.3 kD. (B) Loading of all proteins per sample visualized by Ponceau S staining.

Figure S4. Different *lgg-2* deletion alleles exhibit similar phenotypes.

(A-C) Assays described in Figure 4 were performed with another knockout allele of *lgg-2* in the HW background. (A) *N. ironsii* clearance in *lgg-2*(*jy44)* mutants (orange line) and *lgg-2(jy45)* mutants (purple line). Thick lines represent average values from two independent experiments; each replicate is shown with dotted line. HW and N2 wild-type controls are shown in green and gray lines, respectively. (B) Box-and-whiskers plot shows similar *N. ironsii* infection rate between *lgg-2*(*jy44)* and *lgg-2(jy45)* alleles (3 hpi). Only infected animals from two experiments were included. Each box represents 50% of the data closest to the median value (line in the box). Whiskers span the values outside of the box. Note that mean value for HW sample is four sporoplasms per animal and that it overlaps with the upper boundary of the box. (C) *lgg2(jy44)* and *lgg-2(jy45)* mutants show similar feeding rate. Feeding assay was performed in triplicate, 50 animals were analyzed per strain per experiment. (B, C) A student's t-test was used to calculate p values; $p < 0.001$ is indicated with four asterisks; ns indicates non-significant difference ($p > 0.05$). (A-C) All experiments were performed at 25°C.

Figure S5. Ability to clear infection is similar in wild-type HW animals and *lgg-2* deletion mutants if initial infection rate is similar.

(A, B) *N. ironsii* clearance in HW wild-type (green line) and *lgg-2(jy44)* animals (orange line) is similar if HW wt animals are infected with a higher dose of microsporidia spores than HW *lgg-2(jy44)* mutants, to achieve similar initial intestinal colonization in both strains. (A) *N. ironsii* clearance in HW wild-type animals (green line) and *lgg-2*(*jy44)* mutants (orange line). 100 animals were analyzed per strain at 3 hpi and 20 hpi (x-axis). (B) Box-and-whiskers plot shows

similar *N. ironsii* infection rate between HW wild-type and *lgg-2(jy44)* mutant animals. Each box represents 50% of the data closest to the median value (line in the box). Whiskers span the values outside of the box. Uninfected animals were excluded. A student's t-test was used to calculate *p* values; ns indicates non-significant difference ($p > 0.05$).

References

1. Wang L, Pittman KJ, Barker JR, Salinas RE, Stanaway IB, Williams GD, et al. An Atlas of Genetic Variation Linking Pathogen-Induced Cellular Traits to Human Disease. Cell host & microbe 2018; 24:308-23 e6.
2. Rioux JD, Xavier RJ, Taylor KD, Silverberg MS, Goyette P, Huett A, et al. Genome-wide association study identifies new susceptibility loci for Crohn disease and implicates autophagy in disease pathogenesis. Nature genetics 2007; 39:596-604.
3. Khor B, Gardet A, Xavier RJ. Genetics and pathogenesis of inflammatory bowel disease. Nature 2011; 474:307-17.
4. Lassen KG, Xavier RJ. Genetic control of autophagy underlies pathogenesis of inflammatory bowel disease. Mucosal Immunol 2017; 10:589-97.
5. Benjamin JL, Sumpter R, Jr., Levine B, Hooper LV. Intestinal epithelial autophagy is essential for host defense against invasive bacteria. Cell host & microbe 2013; 13:723-34.
6. Yin Z, Pascual C, Klionsky DJ. Autophagy: machinery and regulation. Microb Cell 2016; 3:588-96.
7. Randow F, Youle RJ. Self and nonself: how autophagy targets mitochondria and bacteria. Cell host & microbe 2014; 15:403-11.
8. Miller C, Celli J. Avoidance and Subversion of Eukaryotic Homeostatic Autophagy Mechanisms by Bacterial Pathogens. J Mol Biol 2016; 428:3387-98.
9. McEwan DG. Host-pathogen interactions and subversion of autophagy. Essays Biochem 2017; 61:687-97.
10. Mitchell G, Isberg RR. Innate Immunity to Intracellular Pathogens: Balancing Microbial Elimination and Inflammation. Cell host & microbe 2017; 22:166-75.
11. Ktistakis NT, Tooze SA. Digesting the Expanding Mechanisms of Autophagy. Trends in cell biology 2016; 26:624-35.
12. Bel S, Pendse M, Wang Y, Li Y, Ruhn KA, Hassell B, et al. Paneth cells secrete lysozyme via secretory autophagy during bacterial infection of the intestine. Science (New York, NY 2017; 357:1047-52.
13. Kuo CJ, Hansen M, Troemel E. Autophagy and innate immunity: Insights from invertebrate model organisms. Autophagy 2018; 14:233-42.
14. Frezal L, Felix MA. C. elegans outside the Petri dish. Elife 2015; 4.

15. Zhang G, Sachse M, Prevost MC, Luallen RJ, Troemel ER, Felix MA. A Large Collection of Novel Nematode-Infecting Microsporidia and Their Diverse Interactions with Caenorhabditis elegans and Other Related Nematodes. PLoS pathogens 2016; 12:e1006093.
16. Vavra J, Lukes J. Microsporidia and 'the art of living together'. Advances in parasitology 2013; 82:253-319.
17. Troemel ER, Felix MA, Whiteman NK, Barriere A, Ausubel FM. Microsporidia are natural intracellular parasites of the nematode *Caenorhabditis elegans*. PLoS biology 2008; 6:2736-52.
18. Szumowski SC, Botts MR, Popovich JJ, Smelkinson MG, Troemel ER. The small GTPase RAB-11 directs polarized exocytosis of the intracellular pathogen N. parisii for fecal-oral transmission from C. elegans. Proceedings of the National Academy of Sciences of the United States of America 2014; 111:8215-20.
19. Bakowski MA, Desjardins CA, Smelkinson MG, Dunbar TA, Lopez-Moyado IF, Rifkin SA, et al. Ubiquitin-mediated response to microsporidia and virus infection in C. elegans. PLoS pathogens 2014; 10:e1004200.
20. Jia K, Thomas C, Akbar M, Sun Q, Adams-Huet B, Gilpin C, et al. Autophagy genes protect against Salmonella typhimurium infection and mediate insulin signaling-regulated pathogen resistance. Proceedings of the National Academy of Sciences of the United States of America 2009; 106:14564-9.
21. Visvikis O, Ihuegbu N, Labed SA, Luhachack LG, Alves AM, Wollenberg AC, et al. Innate host defense requires TFEB-mediated transcription of cytoprotective and antimicrobial genes. Immunity 2014; 40:896-909.
22. Zou CG, Ma YC, Dai LL, Zhang KQ. Autophagy protects C. elegans against necrosis during Pseudomonas aeruginosa infection. Proceedings of the National Academy of Sciences of the United States of America 2014; 111:12480-5.
23. Kirienko NV, Ausubel FM, Ruvkun G. Mitophagy confers resistance to siderophore-mediated killing by Pseudomonas aeruginosa. Proceedings of the National Academy of Sciences of the United States of America 2015; 112:1821-6.
24. Balla KM, Andersen EC, Kruglyak L, Troemel ER. A wild C. elegans strain has enhanced epithelial immunity to a natural microsporidian parasite. PLoS pathogens 2015; 11:e1004583.
25. Reinke AW, Balla KM, Bennett EJ, Troemel ER. Identification of microsporidia host-exposed proteins reveals a repertoire of rapidly evolving proteins. Nat Commun 2017; 8:14023.
26. Cohen LB, Troemel ER. Microbial pathogenesis and host defense in the nematode C. elegans. Current opinion in microbiology 2015; 23:94-101.
27. Irazoqui JE, Urbach JM, Ausubel FM. Evolution of host innate defence: insights from Caenorhabditis elegans and primitive invertebrates. Nature reviews 2010; 10:47-58.
28. Brenner S. The genetics of *Caenorhabditis elegans*. Genetics 1974; 77:71-94.
29. Chang JT, Kumsta C, Hellman AB, Adams LM, Hansen M. Spatiotemporal regulation of autophagy during Caenorhabditis elegans aging. Elife 2017; 6.
30. Manil-Segalen M, Lefebvre C, Jenzer C, Trichet M, Boulogne C, Satiat-Jeunemaitre B, et al. The C. elegans LC3 acts downstream of GABARAP to degrade autophagosomes by interacting with the HOPS subunit VPS39. Dev Cell 2014; 28:43-55.
31. Cuomo CA, Desjardins CA, Bakowski MA, Goldberg J, Ma AT, Becnel JJ, et al. Microsporidian genome analysis reveals evolutionary strategies for obligate intracellular growth. Genome Res 2012; 22:2478-88.

32. Estes KA, Szumowski SC, Troemel ER. Non-lytic, actin-based exit of intracellular parasites from *C. elegans* intestinal cells. PLoS pathogens 2011; 7:e1002227.
33. Paix A, Folkmann A, Rasoloson D, Seydoux G. High Efficiency, Homology-Directed Genome Editing in Caenorhabditis elegans Using CRISPR-Cas9 Ribonucleoprotein Complexes. Genetics 2015; 201:47-54.
34. Perica T, Chothia C. Ubiquitin--molecular mechanisms for recognition of different structures. Current opinion in structural biology 2010; 20:367-76.
35. Melendez A, Levine B. Autophagy in C. elegans. WormBook 2009:1-26.
36. Nguyen TN, Padman BS, Usher J, Oorschot V, Ramm G, Lazarou M. Atg8 family LC3/GABARAP proteins are crucial for autophagosome-lysosome fusion but not autophagosome formation during PINK1/Parkin mitophagy and starvation. The Journal of cell biology 2016; 215:857-74.
37. Alberti A, Michelet X, Djeddi A, Legouis R. The autophagosomal protein LGG-2 acts synergistically with LGG-1 in dauer formation and longevity in C. elegans. Autophagy 2010; 6:622-33.
38. Pollard DA, Rockman MV. Resistance to germline RNA interference in a Caenorhabditis elegans wild isolate exhibits complexity and nonadditivity. G3 (Bethesda) 2013; 3:941-7.
39. Mitchell G, Cheng MI, Chen C, Nguyen BN, Whiteley AT, Kianian S, et al. Listeria monocytogenes triggers noncanonical autophagy upon phagocytosis, but avoids subsequent growth-restricting xenophagy. Proceedings of the National Academy of Sciences of the United States of America 2018; 115:E210-E7.
40. Hayman JR, Southern TR, Nash TE. Role of sulfated glycans in adherence of the microsporidian Encephalitozoon intestinalis to host cells in vitro. Infection and immunity 2005; 73:841-8.
41. Han B, Polonais V, Sugi T, Yakubu R, Takvorian PM, Cali A, et al. The role of microsporidian polar tube protein 4 (PTP4) in host cell infection. PLoS pathogens 2017; 13:e1006341.

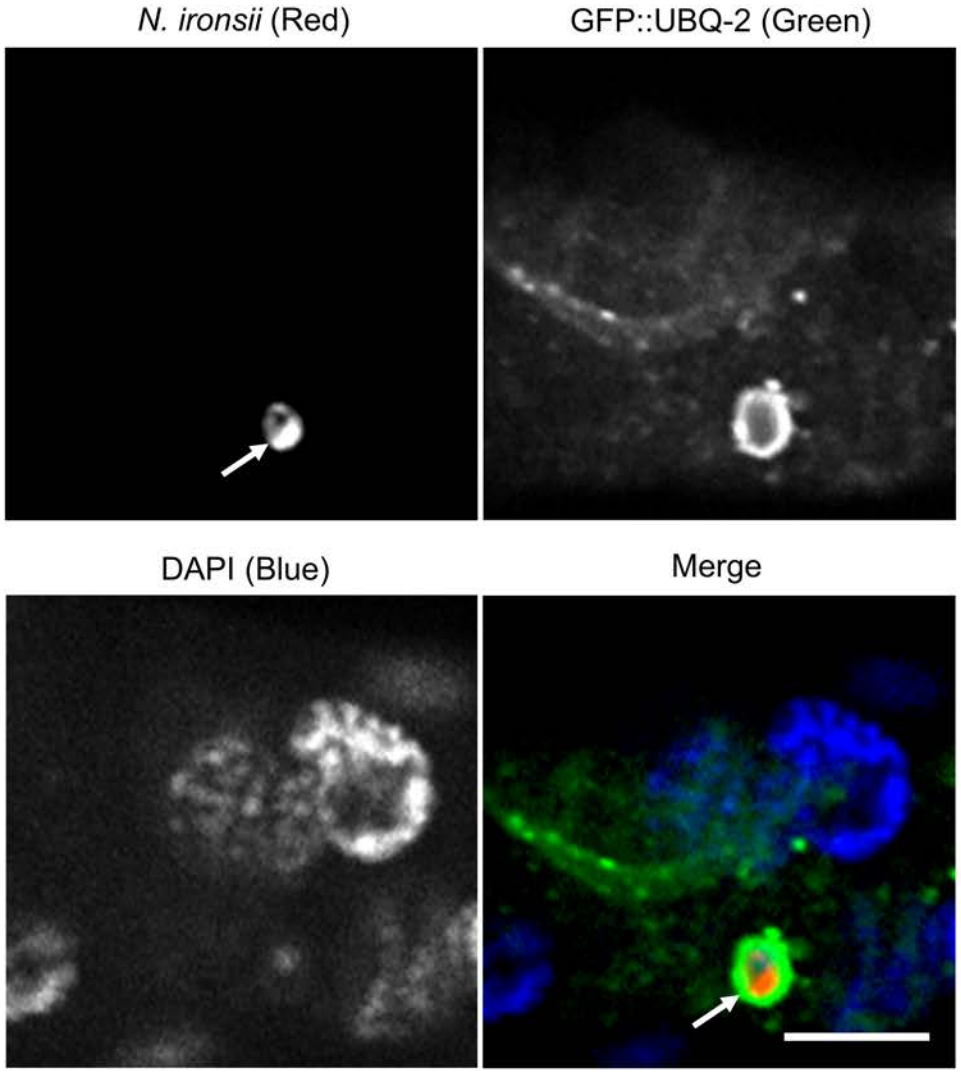
A
N. ironsii (Red)
GFP::UBQ-2 (Green)
DAPI (Blue)
Merge

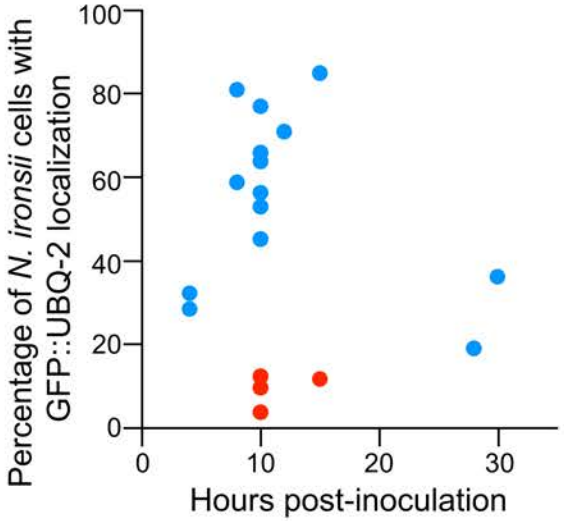
B
Percentage of N. ironsii cells with GFP::UBQ-2 localization
100
80
60
40
20
0
0
10
20
30
Hours post-inoculation

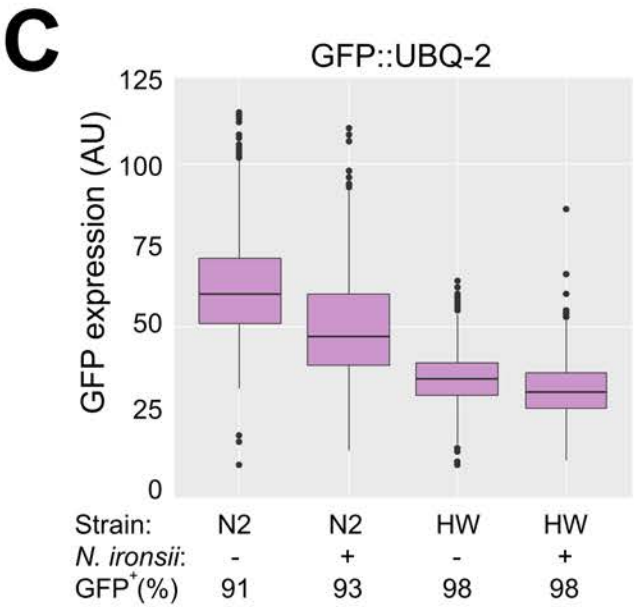
C
GFP::UBQ-2
GFP expression (AU)
125
100
75
50
25
0
Strain: N2 N2 HW HW
N. ironsii: - + - +
GFP+(%) 91 93 98 98

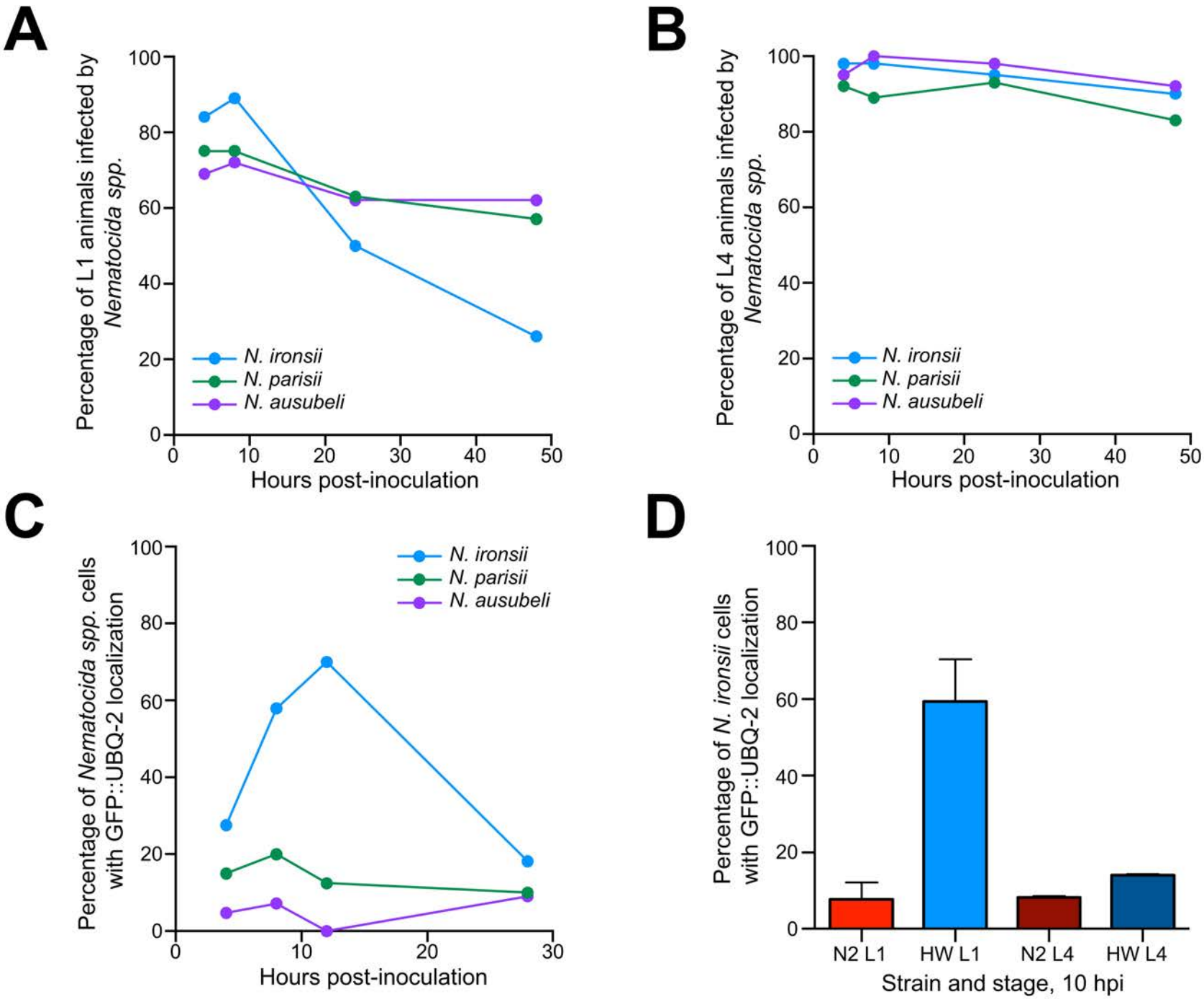
A
Percentage of L1 animals infected by Nematocida spp.
Hours post-inoculation
N. ironsii
N. parisii
N. ausubeli
B
Percentage of L4 animals infected by Nematocida spp.
Hours post-inoculation
N. ironsii
N. parisii
N. ausubeli
C
Percentage of Nematocida spp. cells with GFP::UBQ-2 localization
Hours post-inoculation
N. ironsii
N. parisii
N. ausubeli
D
Percentage of N. ironsii cells with GFP::UBQ-2 localization
N2 L1
HW L1
N2 L4
HW L4
Strain and stage, 10 hpi

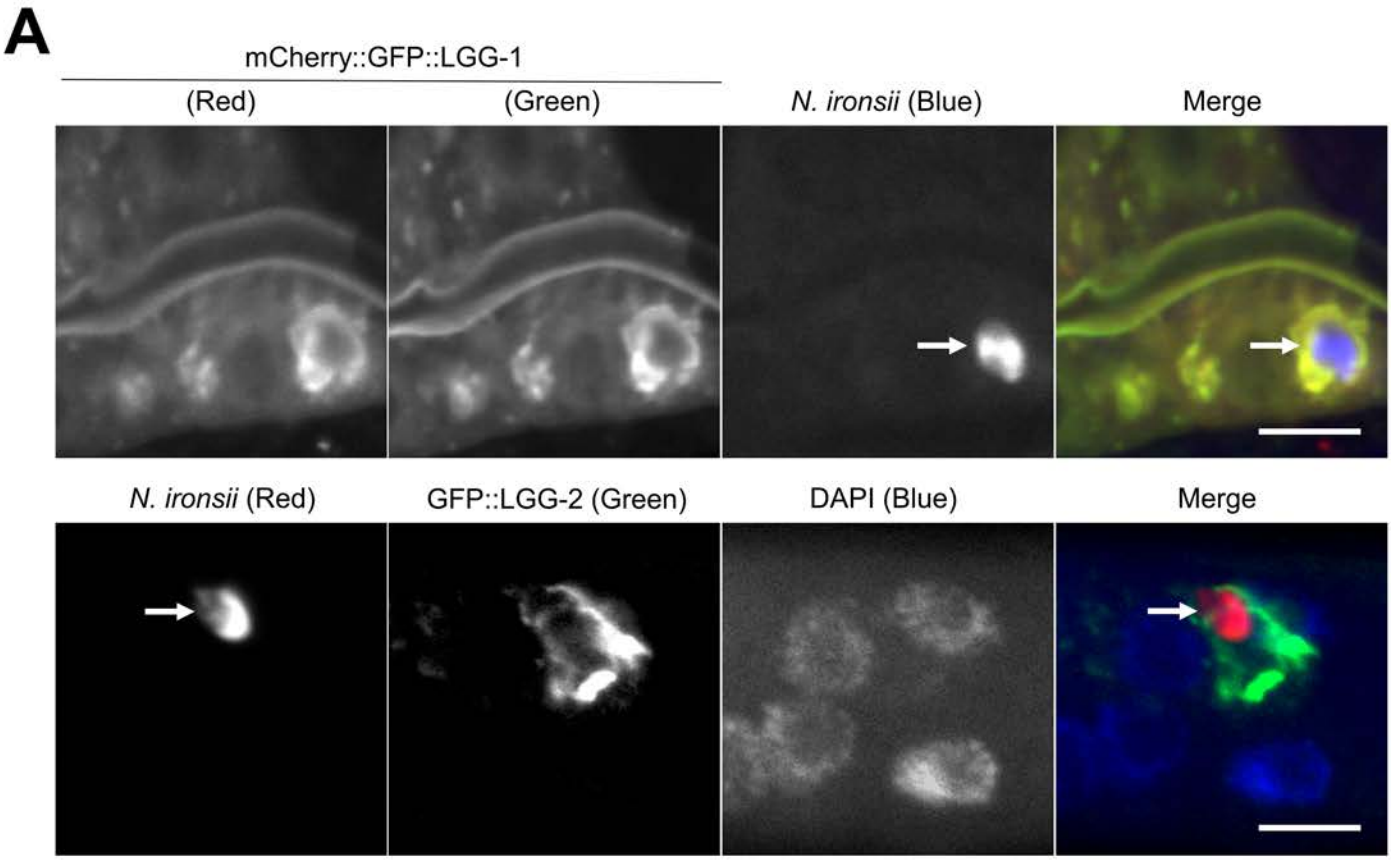
A
mCherry::GFP::LGG-1
(Red)
(Green)
N. ironsii (Blue)
Merge
N. ironsii (Red)
GFP::LGG-2 (Green)
DAPI (Blue)
Merge

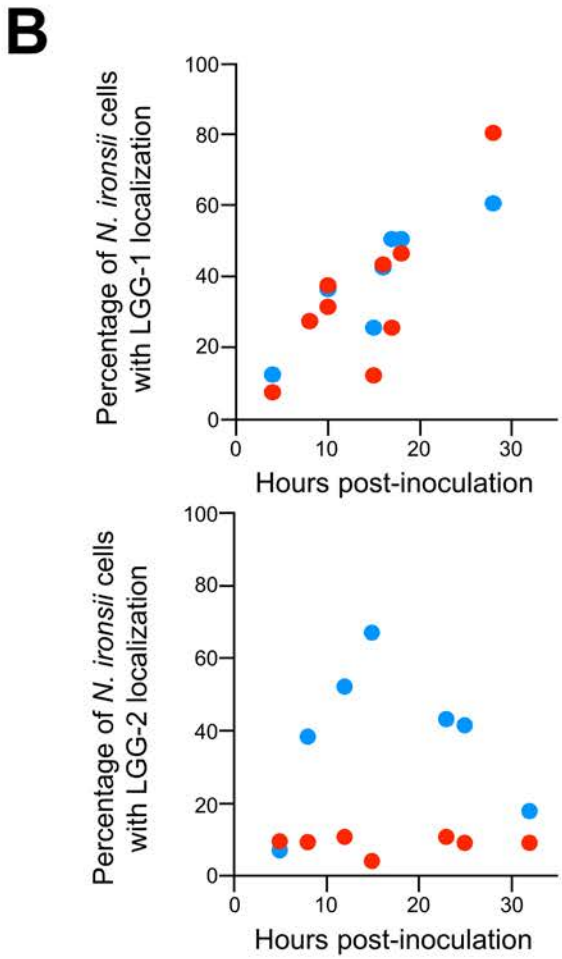
B
Percentage of N. ironsii cells with LGG-1 localization
Hours post-inoculation
Percentage of N. ironsii cells with LGG-2 localization
Hours post-inoculation

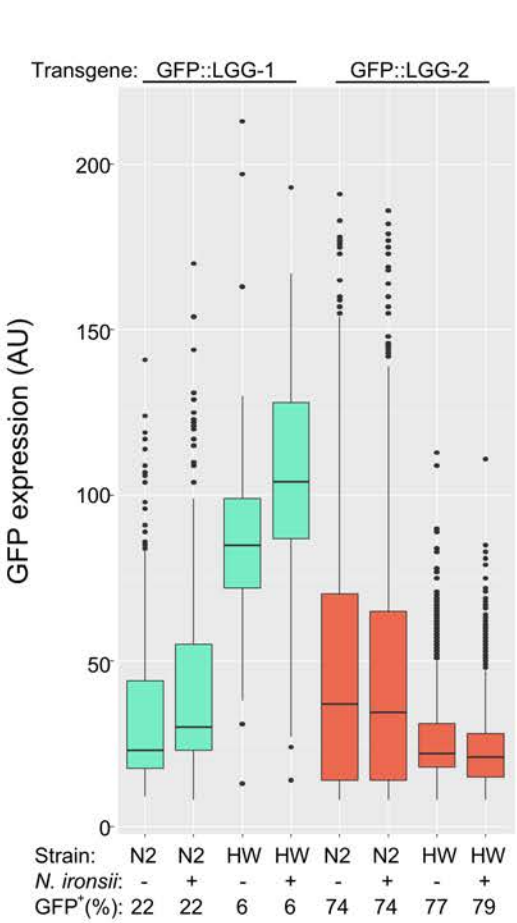
C
Transgene: GFP::LGG-1 GFP::LGG-2
GFP expression (AU)
Strain: N2 N2 HW HW N2 N2 HW HW
N. ironsii: - + - + - + - +
GFP+(%): 22 22 6 6 74 74 77 79

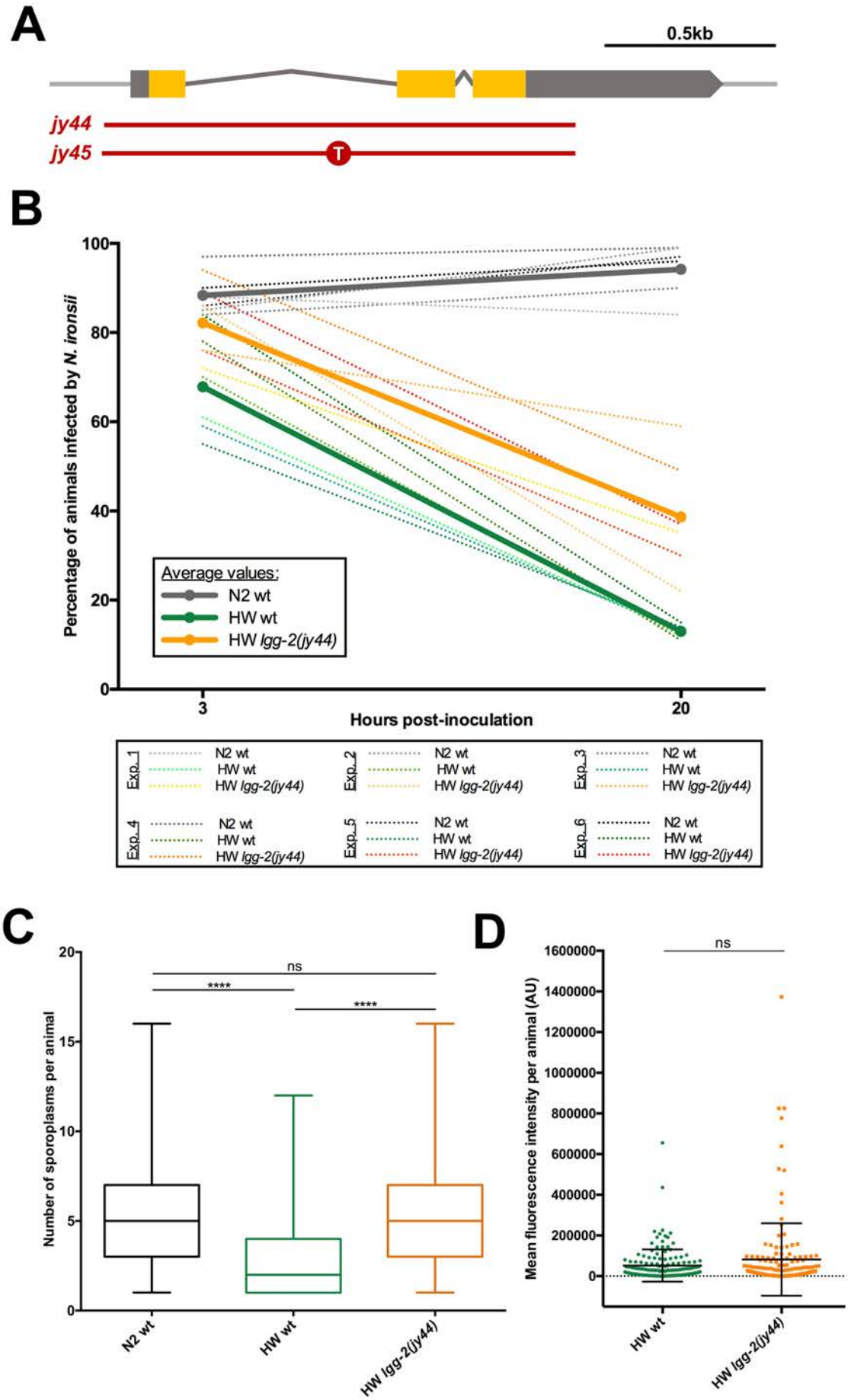
A
0.5kb
jy44
jy45
T
B
Percentage of animals infected by N. ironsii
Hours post-inoculation
Average values:
N2 wt
HW wt
HW lgg-2(jy44)
Exp. 1
Exp. 2
Exp. 3
Exp. 4
Exp. 5
Exp. 6
C
Number of sporoplasms per animal
ns
****
****
N2 wt
HW wt
HW lgg-2(jy44)
D
Mean fluorescence intensity per animal (AU)
ns
HW wt
HW lgg-2(jy44)

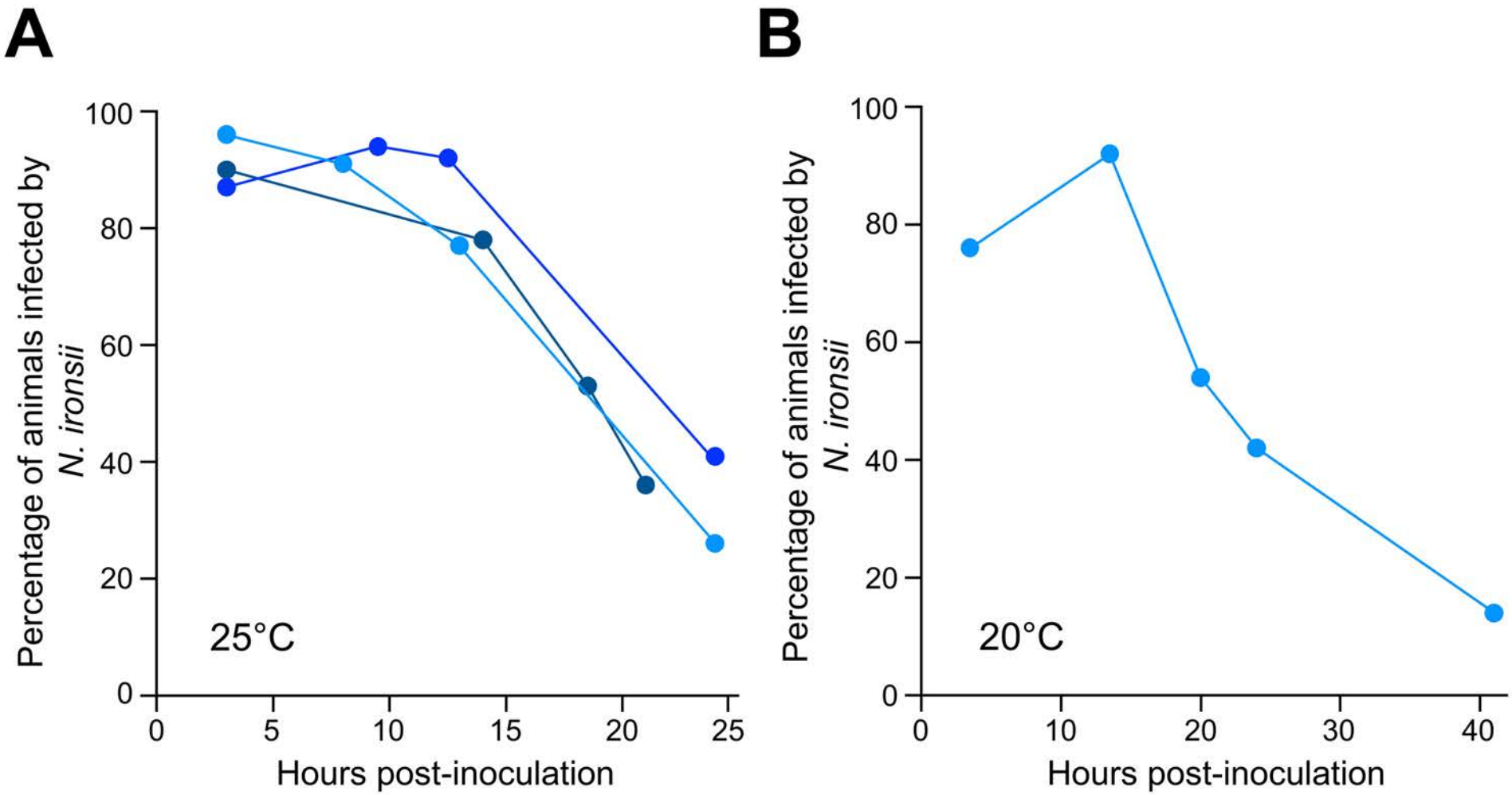
A
B
Percentage of animals infected by N. ironsii
Hours post-inoculation
25°C
20°C
0
20
40
60
80
100
0
5
10
15
20
25
30
40

Microsporidia infection
of British “N2”
C. elegans

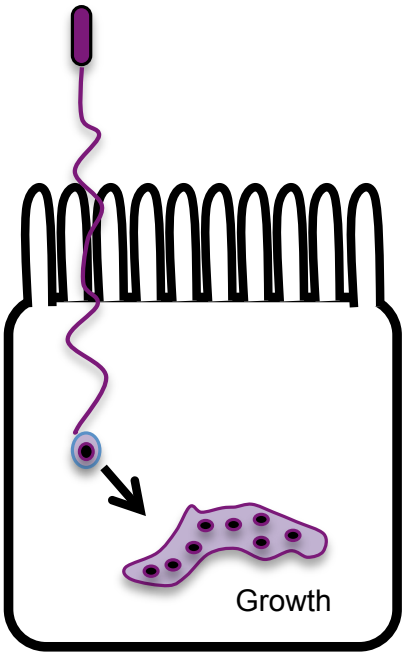

- Does not clear infection
- Lo Ub on parasite
- Lo LGG-2/LC3 on parasite

Microsporidia infection
of Hawaiian “HW”
C. elegans

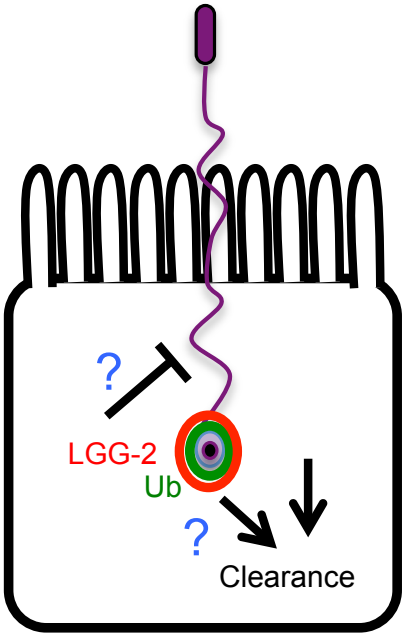

- Clears infection as L1, not L4
- Hi Ub on parasite in L1, not L4
- Hi LGG-2/LC3 on parasite
- Non-LGG-2 pathway drives clearance
- LGG-2 inhibits colonization

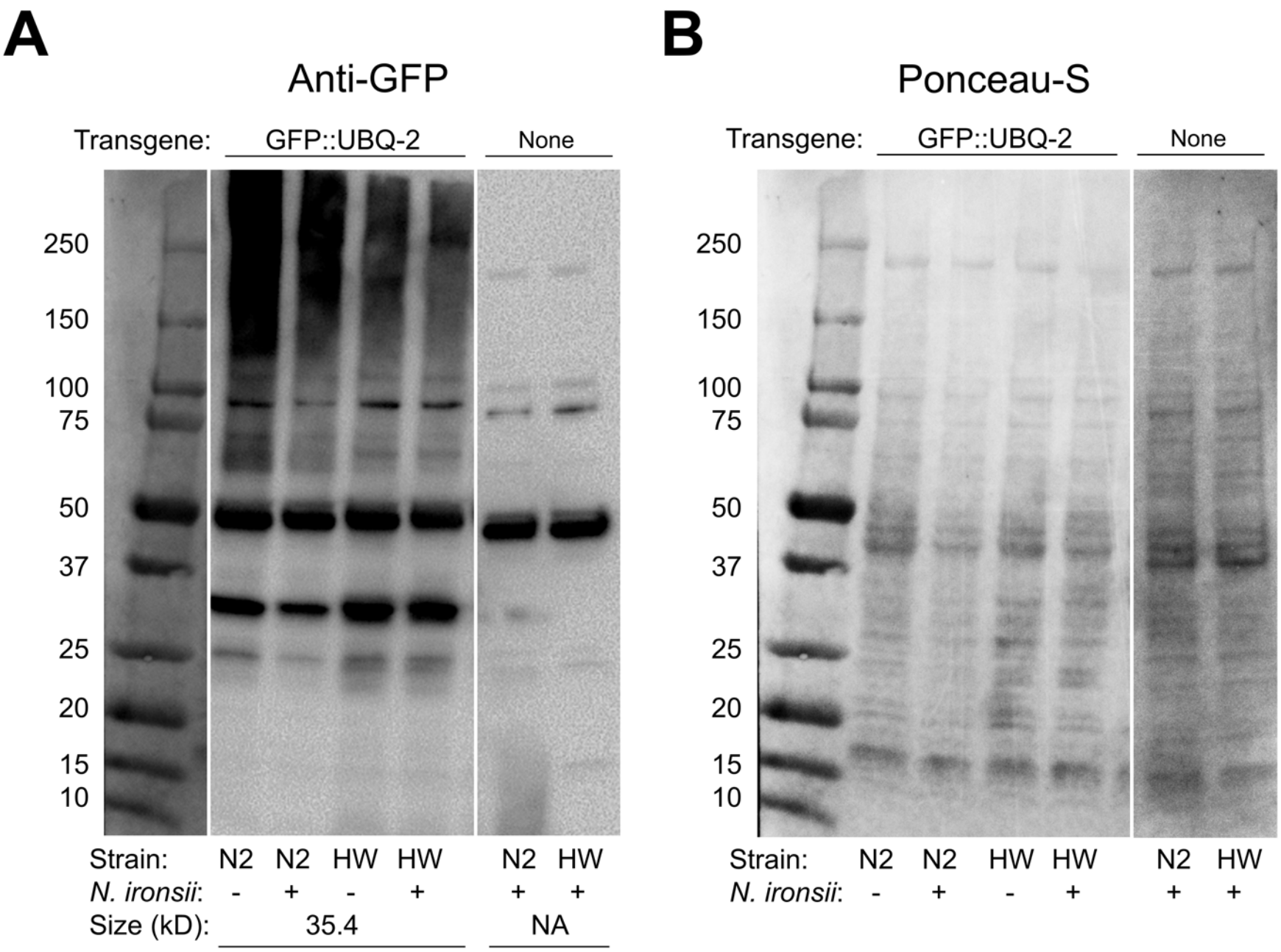
A
Anti-GFP
Transgene:
GFP::UBQ-2
None
250
150
100
75
50
37
25
20
15
10
Strain:
N2
N2
HW
HW
N2
HW
N. ironsii:
-
+
-
+
+
+
Size (kD):
35.4
NA
B
Ponceau-S
Transgene:
GFP::UBQ-2
None
250
150
100
75
50
37
25
20
15
10
Strain:
N2
N2
HW
HW
N2
HW
N. ironsii:
-
+
-
+
+
+

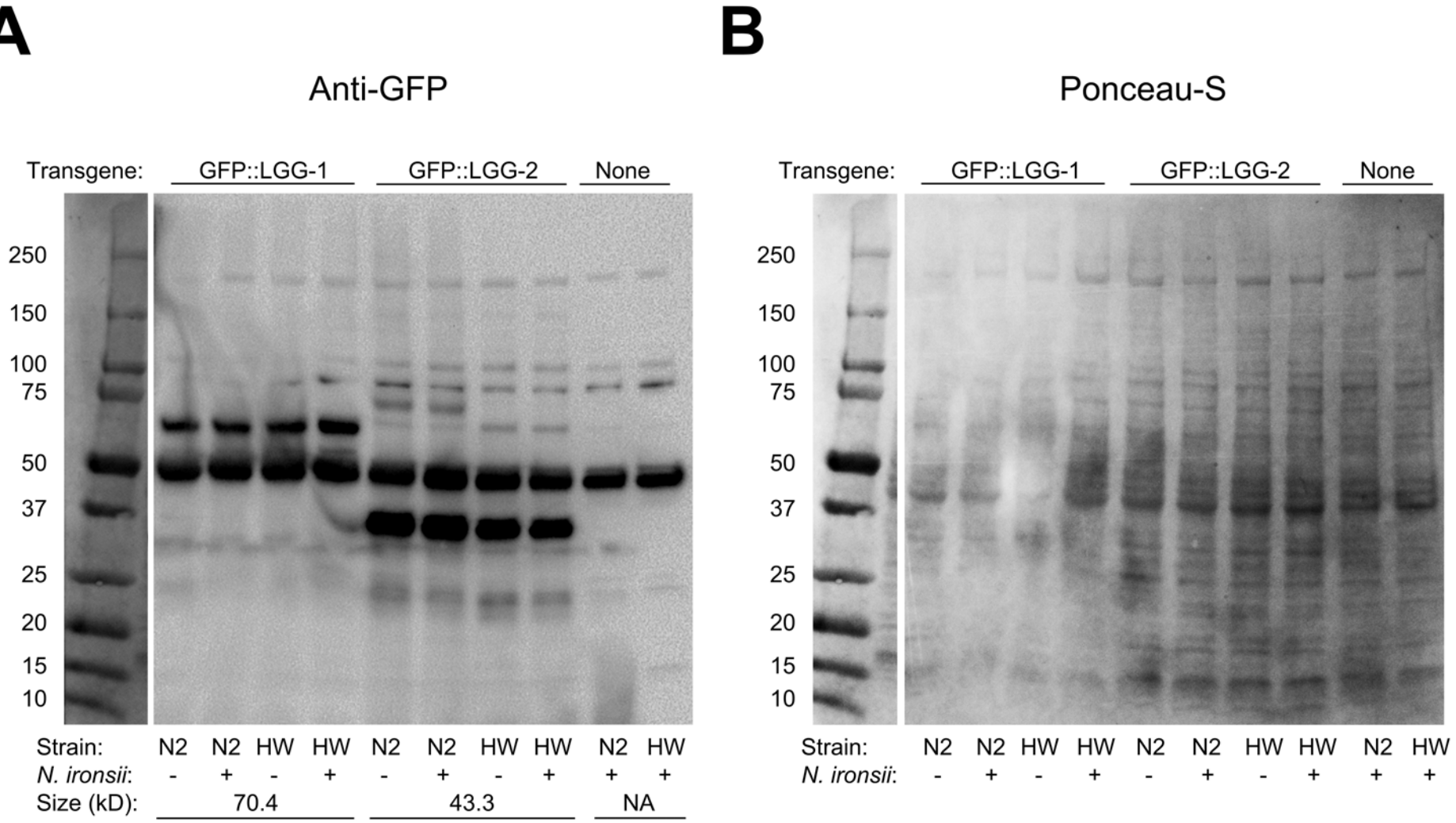
A
Anti-GFP
Transgene:
GFP::LGG-1
GFP::LGG-2
None
250
150
100
75
50
37
25
20
15
10
Strain:
N2 N2 HW HW N2 N2 HW HW N2 HW
N. ironsii:
- + - + - + - + + +
Size (kD):
70.4
43.3
NA
B
Ponceau-S
Transgene:
GFP::LGG-1
GFP::LGG-2
None
250
150
100
75
50
37
25
20
15
10
Strain:
N2 N2 HW HW N2 N2 HW HW N2 HW
N. ironsii:
- + - + - + - + + +

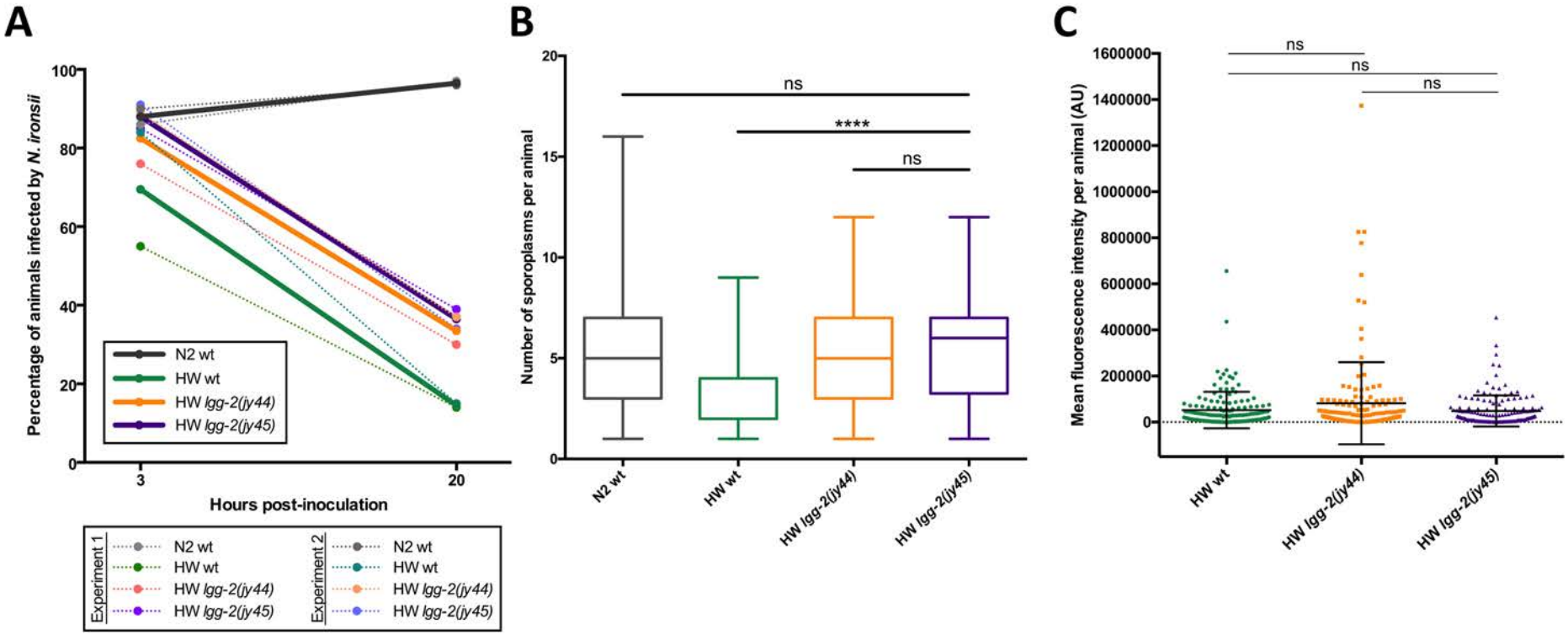
A
Percentage of animals infected by N. ironsii
100
80
60
40
20
0
3
20
Hours post-inoculation
N2 wt
HW wt
HW lgg-2(jy44)
HW lgg-2(jy45)
Experiment 1
N2 wt
HW wt
HW lgg-2(jy44)
HW lgg-2(jy45)
Experiment 2
N2 wt
HW wt
HW lgg-2(jy44)
HW lgg-2(jy45)
B
Number of sporoplasms per animal
20
15
10
5
0
ns
****
ns
N2 wt
HW wt
HW lgg-2(jy44)
HW lgg-2(jy45)
C
Mean fluorescence intensity per animal (AU)
1600000
1400000
1200000
1000000
800000
600000
400000
200000
0
ns
ns
ns
HW wt
HW lgg-2(jy44)
HW lgg-2(jy45)

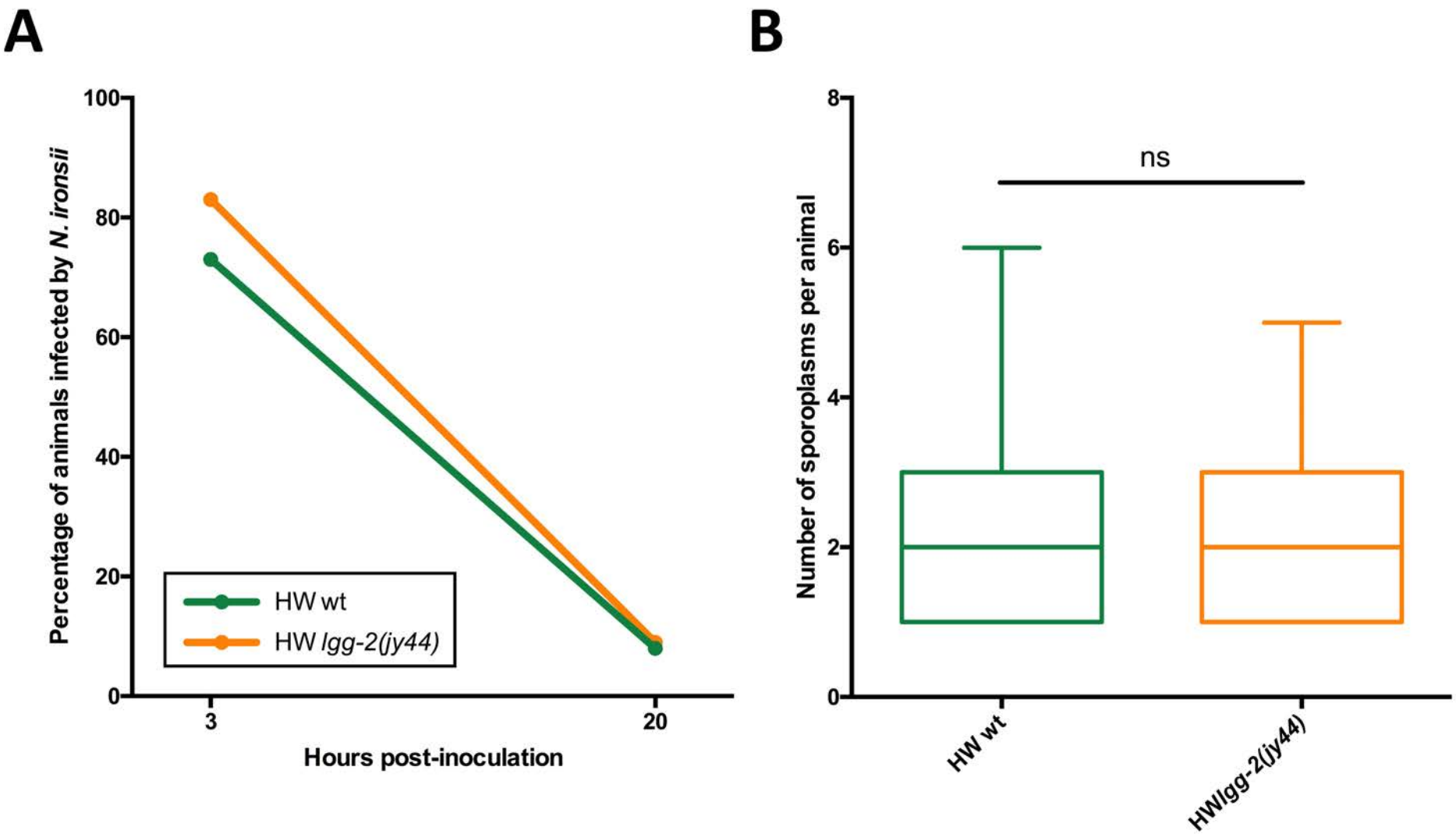
A
100
80
60
40
20
0
Percentage of animals infected by N. ironsii
HW wt
HW lgg-2(jy44)
3
20
Hours post-inoculation
B
8
6
4
2
0
Number of sporoplasms per animal
ns
HW wt
HWlgg-2(jy44)